

NOVEL ACOUSTIC-WAVE MICROMIXER

Vibhu Vivek, Yi Zeng and Eun Sok Kim*

Department of Electrical Engineering, University of Hawaii at Manoa, Honolulu, HI 96822

*Present Address: Department of EE-Electrophysics, University of Southern California, Los Angeles, CA 90089

ABSTRACT

This paper describes a novel Fresnel Annular Sector Actuator (FASA) and FASA-based micromixers built on PZT substrate. This actuator generates strong lateral acoustic thrusts in liquid, and is very effective in micromixing fluids. Almost any lateral fluidic motion can be produced with appropriate electrode patterns on FASA and with a combination of various FASA elements. We have developed the following three micromixers based on FASA elements: overlap design, four-sector design and six-sector design. Experimental results obtained on the fabricated FASA and micromixers confirm the theory and simulation.

INTRODUCTION

Microfluidic processing systems need to transport and/or mix two or more kinds of fluids of accurately controlled amount in reasonable period of time. Since many microfluidic devices are fabricated in planar lithographic environment, most of the macroscopic approaches for fluid mixing like turbulence and mechanical actuation are inapplicable at microscopic levels. And using heat for mixing is not desirable for mixing temperature sensitive fluids (such as DNA sample). A mechanical plunger with a push-pull operational mode is effective for mixing fluids, but only as long as the fluid height is greater than 500 μm while the fluid-surface area is around $\text{mm}^2 - \text{cm}^2$ range.

It has been reported that focused acoustic waves (generated by annular rings of half-wave-band sources made of piezoelectric thin film and electrodes sitting on a diaphragm) are effective in generating fluidic motion [1]. But when the fluid height is reduced to 100 μm range while the fluid-surface area remains in $\text{mm}^2 - \text{cm}^2$ range, there must be much stronger lateral acoustic pressure to push and pull the fluid for mixing. Thus, we have invented Fresnel Annular Sector Actuator (FASA). This paper describes the theory, simulation and experimental results of FASA.

THEORY

The operating principle of FASA is based on the self-focusing acoustic-wave transducer, which focuses acoustic waves (generated by annular rings of half-wave-band sources made of piezoelectric thin film and electrodes sitting on a diaphragm) through constructive wave interference [1]. In the transducer, when RF power is applied between the electrodes (sandwiching the piezoelectric film) with its frequency corresponding to the thickness mode resonance of the piezoelectric film, strong acoustic waves are generated over the electrode areas, and interfere with each other as they propagate in the fluid. With a proper design of the annular electrodes, we can achieve wave focusing without any acoustic lens.

When the complete annular rings are broken into segments of different angles, there are proportionate changes in the vertical and lateral acoustic-potential profiles.



Figure1 Fresnel Annular Sector Actuator (FASA) transducer: the basic cell.

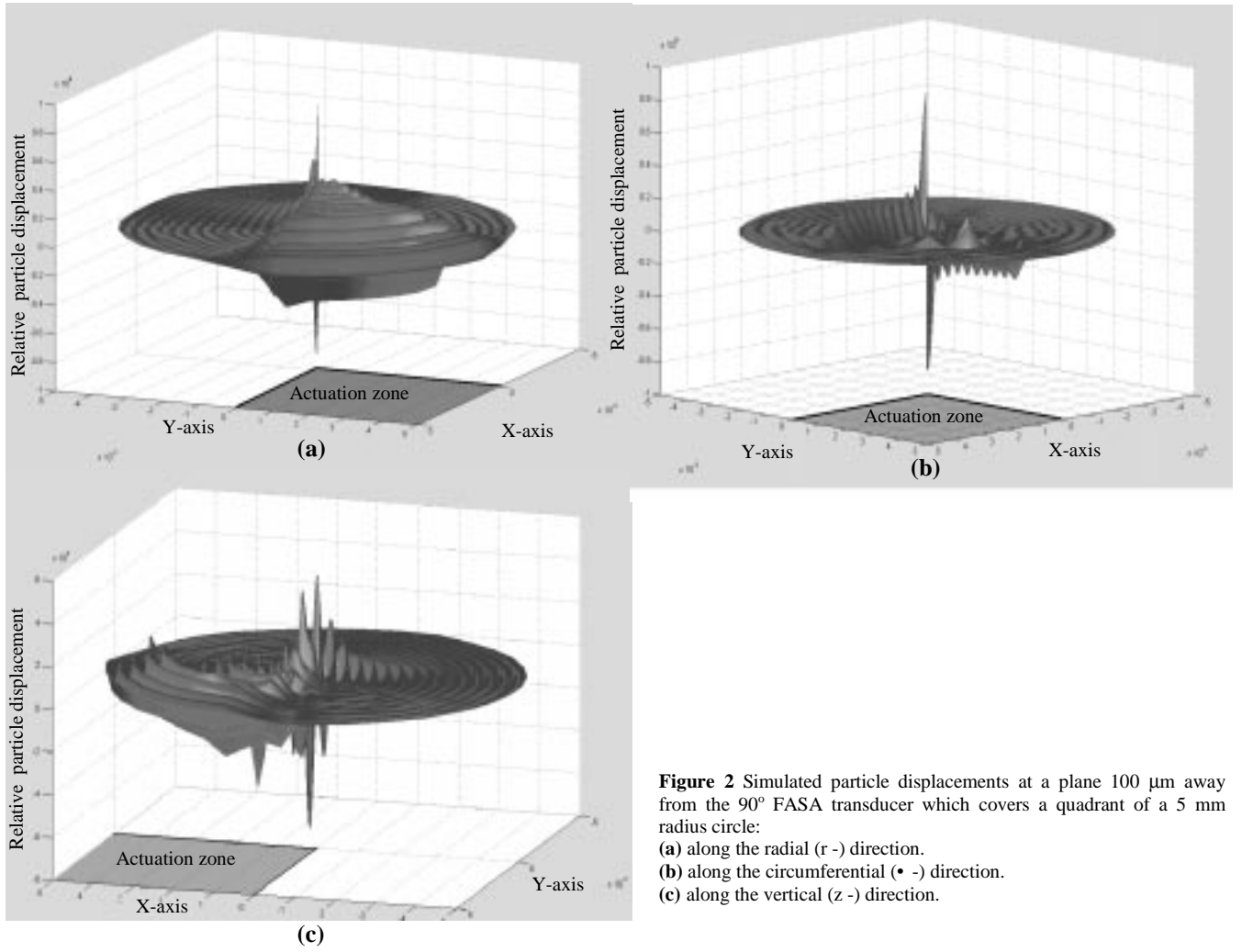


Figure 2 Simulated particle displacements at a plane $100 \mu\text{m}$ away from the 90° FASA transducer which covers a quadrant of a 5 mm radius circle:

- (a) along the radial (r -) direction.
- (b) along the circumferential (ϕ -) direction.
- (c) along the vertical (z -) direction.

With the angle of the sector getting smaller, the gradient of the lateral acoustic potential becomes larger, while the vertical potential profile becomes more distributed. Thus, we have invented a so called 90° FASA on a PZT substrate as shown in Fig. 1. The electrode patterns for the top and bottom electrodes are designed to produce a very high lateral acoustic-potential gradient.

Figure 2 shows the simulation results of particle displacements (in r , ϕ , and z directions in the cylindrical coordinate system) at the designed focal plane of $100 \mu\text{m}$ from the 90° FASA transducer which covers a quadrant of a 5 mm radius circle. From Fig. 2a, which shows the particle displacement in the radial direction, we observe the ratio of the center peak to the next side lobe to be 5:1 with the center peak having a relative value of 1×10^9 . On the other hand, Fig. 2c (which plots the particle displacement in the vertical or z - direction) shows more distributed acoustic field with

the ratio of the center peak to the next side lobe being 3:1 and the center peak being only about 6×10^8 relative value. Comparing these two simulations, we see that for shallow water (with height being much smaller than any one dimension of a square surface area), the acoustic potential gradient is stronger in the radial direction than in the vertical direction. Also, in Figure 2b (which shows the particle displacement in the ϕ - direction which is related to a rotational force), we see two peaks with 180° phase difference around the circular-plane center. This means that at the local point the main flow is separated into two with opposite directions. These two flows create the flow pattern that we want for an efficient micromixing.

Figure 3 shows a simulated vector flow of particle displacement at a plane that is about $150 \mu\text{m}$ above the 90° FASA. From this simulation, we observe two loops and the directional shoot-out of the fluid at the center of the figure (i.e., the 90° corner of the 90°

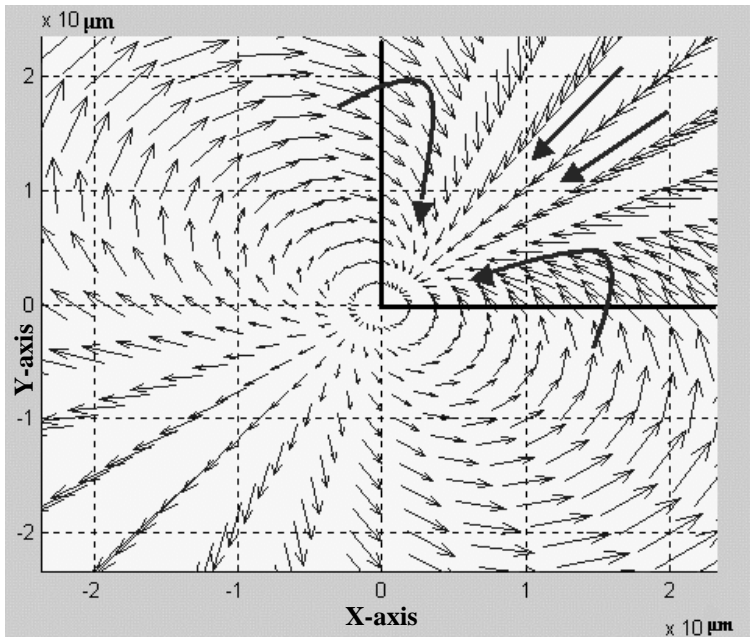


Figure 3 Simulated vector field of particle displacements at a plane 150 μm away from the transducer.

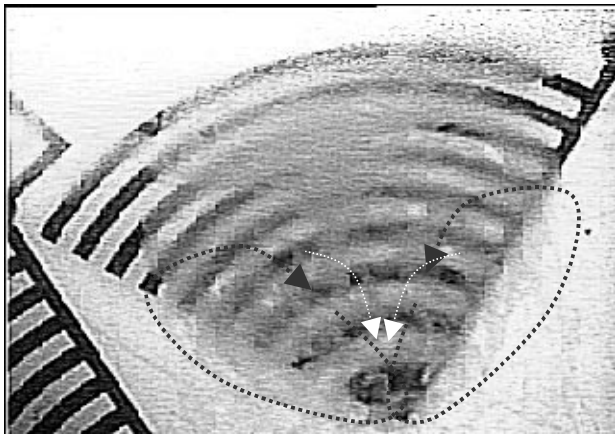


Figure 5 Snapshot over a working Six-Sector Cornered Micromixer showing the liquid flow profile in accordance with the vector field shown in Fig. 3.

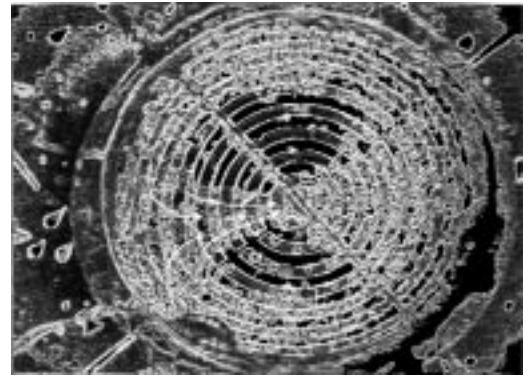
FASA), and consider this movement as a driving pattern. The flow pattern near the center is very strong, and dominates the fluid flow in the area.

MICROMIXER DESIGN

We have come up with the following three designs of micromixer using the 90° FASA: overlap design, four-sector design and six-sector design. The overlap design



4(a)



4(b)

Figure 4-a Snapshot showing the working of an Overlapping FASA Micromixer at its designed focal length (100 • m). The diameter of the largest annular ring for this design is 6727 • m

Figure 4-b Enhanced image using the 'Thin edge transform'. The arrows indicate the direction of fluid flow.

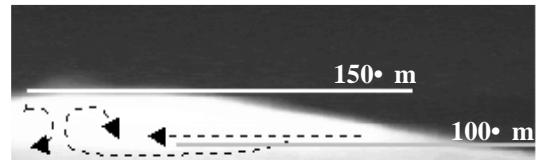


Figure 6 Side view of the fluid on a 90° FASA showing the vertical motions near the 90° corner along with the lateral flow.

has top and bottom electrodes segmented such that the overlap area under actuation at any given time is 90° , thus making a total of 4 overlaps. The switching schematic is shown in Fig. 7a. In the four-sector design (Fig. 7b), there are four isolated sectors placed away from the center along with 4-corner sectors to eliminate dead-zone at the corners. In the six-sector design (Fig. 7c), we place six segments in the middle for more area coverage. The predicted fluid flow profiles are also shown in Figs. 7b and 7c.

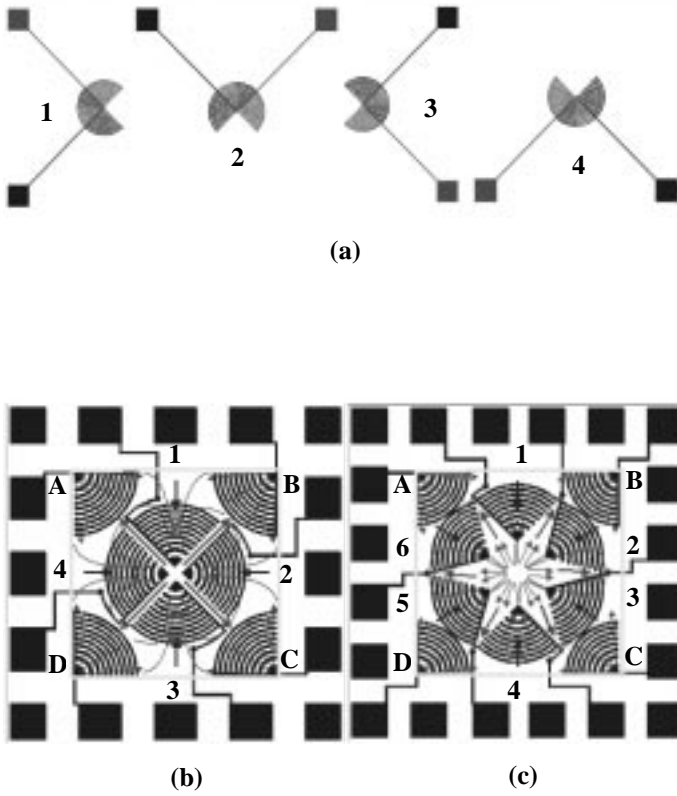


Figure 7 (a) Switching schematics of the Overlap Micromixer. (b) Fluid flow profiles for Four-sector Cornered FASA Micromixer. (c) Fluid flow profiles for Six-sector Cornered FASA Micromixer.

We have made the switching network, taking into account the interference and canceling effects among the sectors, which would happen if we operate the sectors at the same time. For the overlapping micromixer, the operating sequence is described Fig. 7a. For the four-sector design, an actuating cycle consists of four periods with the following order: first, A1B; second, B2C; third, C3D; and then fourth, D4A, where A, B, C, and D are the corner elements; 1, 2, 3, and 4 are the center elements as illustrated in Figs. 7b and 7c. While the denoted three sectors are actuated at the same time (e.g., A1B), they together form a complete loop, as illustrated in Fig. 7b. For the six-sector cornered design, the actuating cycle is as follows: first, A1B; then, B23C; then, C4D; then, D56A, in that order. With all these switching schemes different micromixing motion can be achieved for various kinds fluids.

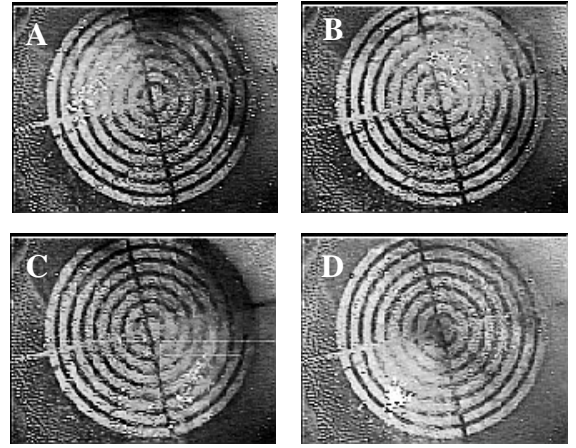


Figure 8 Snapshots of the rotating sequence of the Overlap Micromixer.

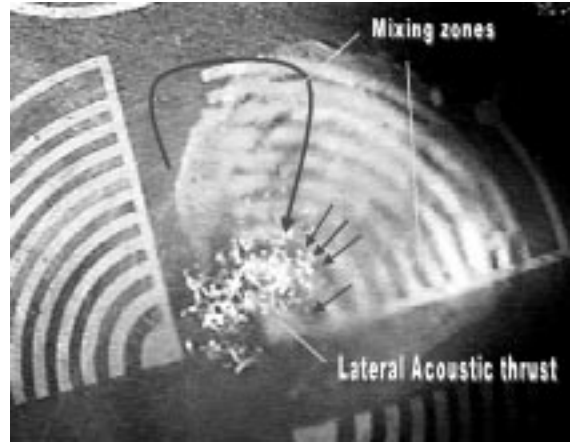


Figure 9 Snapshot of the flow pattern of the microspheres in liquid that resides over FASA.

FABRICATION

The fabrication process for the FASA micromixers (illustrated in Fig. 10) is as follows. With a front-to-backside alignment, we pattern Aluminum layer (0.9 μm thick) on both sides of the PZT into top and bottom FASA electrodes totally overlapping each other. We form 5000 μm wide and 100 μm tall cavity walls (around the transducer as shown in Fig. 12) with the SU-8. Figure 11 shows photos of three types of fabricated FASA micromixers.

EXPERIMENTAL RESULTS

The fabricated devices are tested with a set-up shown in Fig. 12 where 4.5MHz sinusoidal signal is modulated with a square wave from a function generator. After being amplified, the signal is sent to a

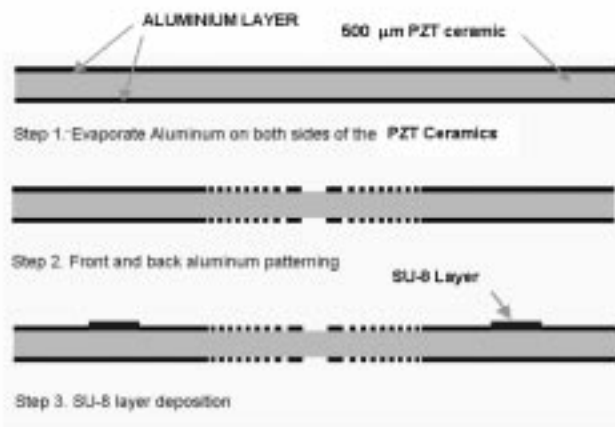


Figure 10 Fabrication steps of the FASA Micromixer.

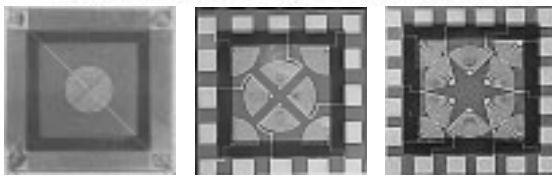


Figure 11 (Left) Overlap Micromixer,
(Middle) Four-Sector Cornered Micromixer,
(Right) Six-Sector Cornered Micromixer.

switching network, which distributes the signal to the individual sectors according to the actuating sequence described in the previous section. Currently, we use an average power of about 100 mW to actuate each sector. Most of that power is reflected due to electrical impedance mismatch, and the actual power delivered to each sector is much lower than 100 mW. With such a low power level, there is no heating effect to the mixing liquids.

To facilitate observation of the mixing effects, we immerse polystyrene microspheres (10 μm in diameter) in the liquid. Figure 4 shows the original snapshot and enhanced image of a working overlapping FASA micro-mixer. Just as predicted in the vector flow simulations, the water flow (viewed clearly with microsphere movement) demonstrates the simulated pattern. Figure 5 is another snapshot taken from a working six-sector cornered micromixer. In both cases, we observe the expected flow pattern at the designed water level.

Figure 6 is a photo taken on a working FASA from a cross-sectional point of view. The vertical movement is clear in this view angle. At the center the water level is slightly larger than 100 μm . (We observe when a sector is actuated, the water is gathering at the high-energy area, which makes the water level profile

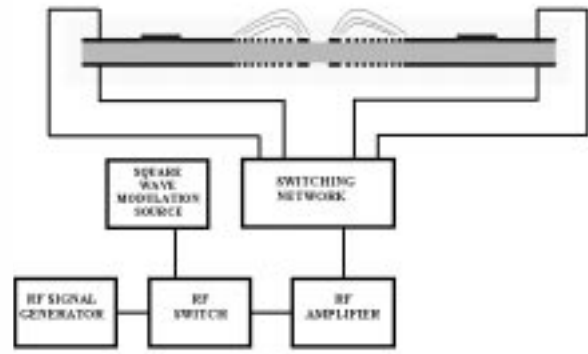


Figure 12 Schematic Representation of the test setup.

uneven.) While in the sector the displacement is in general upward, outside the sector the displacement is downward in general, as expected from the simulation on the z displacement (Fig. 2c). Note the two peaks with 180° phase difference, which indicate two flows in opposite directions near the center. The vertical fluidic flows make fluids at different elevation levels be mixed effectively.

The mixing patterns of an overlap micromixer under switching are shown in Figure 8, which is composed of four consecutive snapshots for an operating cycle comprising of four actuation periods. It can be seen that in each actuation period, the liquid on top of the corresponding 90° FASA element undergoes micromixing. Another snapshot shown in Fig. 9 is taken from a four-sector cornered device, and we see the lateral acoustic thrust and the mixing zones where the microspheres are evenly rotated.

SUMMARY

In this paper, we describe the theory, simulation and experimental results on FASA and FASA-based micromixers fabricated on a PZT substrate. We demonstrate that the FASA and micromixers are very effective in mixing liquids over a relatively large area (in $\text{mm}^2 - \text{cm}^2$ range) when the liquid height is in 100

μm range. Since the FASA-based device produces strong acoustic thrusts in fluid without any heat, it is very attractive in micromixing temperature-sensitive fluids. Other advantages include its ability for a non-intrusive mixing (i.e., the device does not have to be in direct contact with mixing fluids), low power consumption, zero-dead-volume mixing, and inherently fast operation.

ACKNOWLEDGEMENT

The authors wish to thank Dr. Fred J. von Preissig and Dai Huang of UH-MEMS group for helps in the theoretical modeling and computer simulation, respectively. This material is based upon work supported by Naval EOD Technology Division under contract N00174-98-K-0016.

REFERENCES

1. X. Zhu and E.S. Kim, "Microfluidic Motion Generation with Acoustic Waves," *Sensors and Actuators: A. Physical*, vol. 66/1-3, pp. 355-360, April 1998.
2. H. Wang and E.S. Kim, "Ejection Characteristics of Micro machined Acoustic-Wave Liquid Ejector" *The 10th International conference on solid-state Sensors and Actuators* pp.1784-1788.
3. G.S. Kino "Acoustic Wave, Design Imaging & Analog Signal Processing" *Prentice-Hall Inc.*